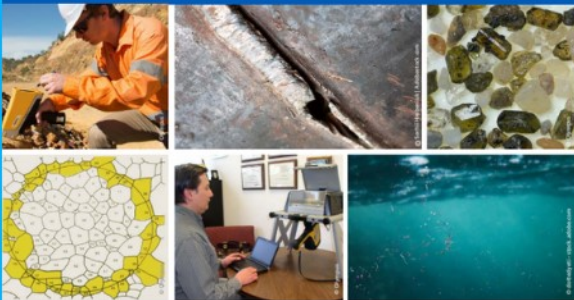




2nd Advanced Optical Metrology Compendium

Advanced Optical Metrology

Geoscience | Corrosion | Particles | Additive Manufacturing: Metallurgy, Cut Analysis & Porosity



EVIDENT
OLYMPUS

WILEY

The latest eBook from **Advanced Optical Metrology**.
Download for free.

This compendium includes a collection of optical metrology papers, a repository of teaching materials, and instructions on how to publish scientific achievements.

With the aim of improving communication between fundamental research and industrial applications in the field of optical metrology we have collected and organized existing information and made it more accessible and useful for researchers and practitioners.

EVIDENT
OLYMPUS

WILEY

4D Printing-Encapsulated Polycaprolactone–Thermoplastic Polyurethane with High Shape Memory Performances

Davood Rahmatabadi, Mohammad Aberoumand, Kianoosh Soltanmohammadi, Elyas Soleyman, Ismaeil Ghasemi, Majid Baniassadi, Karen Abrinia, Mahdi Bodaghi, and Mostafa Baghani**

There are a few shape memory polymers (SMPs) like polylactic acid (PLA) and polyurethane (PU) that are 4D printable, and other SMPs must be synthesized with a complicated chemical lab effort. Herein, considering dual-material extrusion printing and microscopic mechanism behind shape memory effect (SME), bilayer-encapsulated polycaprolactone (PCL)–thermoplastic polyurethane (TPU) shape memory composite structures are 4D printed for the first time. The SME performance is investigated by assessing fixity, shape recovery, stress recovery, and stress relaxation under bending and compression loading modes. PCL, TPU, and melting temperature of PCL play the role of switching phase, net point, and transition temperature, respectively. Due to the destruction and dripping of molten PCL in contact with water, PCL is encapsulated by TPU. Encapsulation successfully solves the challenge of bonding/interface between printed layers, and the results show that the SME performance of the encapsulated structures is higher than bilayer PCL–TPU one's. Experiments reveal that maximum stress recovery in 4D-printed composites remains constant over time. This is a great achievement compared to the previous extrusion-based SMP structures that have great weakness in stress relaxation due to weak and low crystalline fractions and the unraveling of molecular entanglements in semi-crystalline and amorphous thermoplastic SMPs, respectively.


1. Introduction

Shape-memory polymers (SMPs), as the widest and most widely utilized shape memory materials (SMMs), are a group of smart materials that can fix a temporary shape and can return to its original shape by applying proper stimulation.^[1] In recent years,

the 3D printing of SMPs has led to the emergence of the 4D printing term, which was first introduced by Skylar Tibbits.^[2] 4D printing has attracted the attention of researchers because of its benefits and features. In fact, 4D printing is a combination of two advanced and new technologies, 3D printing and smart materials.^[3] In contrast, 4D printing has the advantages of both technologies, including producing complex geometry and shape changing by exerting various stimuli. All additive manufacturing (AM) methods can be used in 4D printing, but polyJet and fused deposition modeling (FDM) have received more attention than others. FDM, as the simplest, cheapest, and most widely used 3D printing method, has a layer-by-layer thermoplastic extrusion mechanism based on the digital model data that is prepared by computer-aided design (CAD).^[4–6] The most convenient 4D printing with FDM is the 3D printing of shape memory thermoplastics, but there are a limited number of printable shape memory thermoplastics in the market, and in recent years, the research materials for 4D printing

have been limited to PLA and PU-based SMPs.^[7–9] In addition, the use of prestrain created during printing (extrusion of molten fiber) and simultaneous programming is another mechanism of 4D printing with FDM. Barletta et al.^[8] investigated the effect of printing parameters including layer thickness, nozzle temperature, velocity, and recovery temperature on 4D printing

D. Rahmatabadi, M. Aberoumand, K. Soltanmohammadi, E. Soleyman, M. Baniassadi, K. Abrinia, M. Baghani
School of Mechanical Engineering
College of Engineering
University of Tehran
Tehran 1417614411, Iran
E-mail: baghani@ut.ac.ir

 The ORCID identification number(s) for the author(s) of this article can be found under <https://doi.org/10.1002/adem.202201309>.

© 2022 The Authors. Advanced Engineering Materials published by Wiley-VCH GmbH. This is an open access article under the terms of the Creative Commons Attribution License, which permits use, distribution and reproduction in any medium, provided the original work is properly cited.

DOI: 10.1002/adem.202201309

I. Ghasemi
Faculty of Processing
Iran Polymer and Petrochemical Institute
Tehran 1497713115, Iran

M. Bodaghi
Department of Engineering
School of Science and Technology
Nottingham Trent University
Nottingham NG11 8NS, UK
E-mail: mahdi.bodaghi@ntu.ac.uk

of PLA structures and their results showed that printed PLA structures have adequate shape memory effect (SME) with a short recovery time. Also, the recovery temperature had the greatest effect on the recovery time, and printing with a higher temperature provides better printability and SME. Bodaghi et al. presented a 4D printing methodology to achieve triple SME with FDM printing of PU-based SMPs^[10] using printing parameters (speed, cooling rate, and layer thickness) and cold programming. They introduced the combination of extrusion of layers (the stretching of the molten fibers during printing) and the difference in their cooling rate to create a prestrain regime. They considered printed structure and its shape after cold loading as the first and second temporary shapes, respectively. In this method, the speed strongly affects the original shape. Hu et al. also used the same method and showed with numerical and experimental methods that the amount of stored prestrain during printing is different in the upper and lower layers and causes self-bending of the PU-based SMP-printed structures after heating and cooling programming, which can be controlled by velocity.^[11] In similar research, it was shown that temperature also affects the amount of shrinkage and internal force stored in printed PU-based SMP, and by printing layers with different temperatures (200 and 220 °C) for a structure and moving the arrangement and geometry of the layers, self-bending direction and shape shifting the structure from 2D to 3D with different geometries are available.^[12] 4D printing of other SMPs has also been developed in recent years. The shape memory properties of 3D-printed PVA with a transition temperature of 37 °C and pharmaceutical applications were investigated.^[13] Also, PETG was introduced as a potential SMP with excellent printing capability, and its shape memory properties were investigated under different conditions (programming temperature, loading mode, and shape memory evaluation).^[14–17] In the meantime, due to the poor performance (stress relaxation caused by weak net points) and the limitations of shape memory thermoplastics, finding a suitable solution for practical 4D printing is still on the agenda and is one of the interesting topics in this field. The reason for this limitation is that the SME is not an inherent property of polymers and to have SME, polymers must have net points or a hard phase and a soft phase which usually requires designing, synthesizing, or blending.^[18,19] Although polymer blending is synthesized with a complicated chemical experimental lab effort, which increases cost and time, it is used as a convenient and cheapest solution in which PLA–TPU is the most common.^[20] However, shape memory polymer blends with excellent printability are also limited^[21–25] and in recent years, limited numbers have been reported. For this reason, there is still a limitation in the number of shape memory polymers and blends, their high cost compared to thermoplastics available in the market, and the need for SMPs with the ability to become filaments and be printed by FDM.

In this study, for the first time, the combination of the microscopic concept of SMPs and multimaterial printing of a thermoplastic elastomer with FDM is introduced to generate a novel 4D printing method without SMP and the extra operation such as synthesis and blending. In addition, this method solves both the challenge of a limited number of shape memory materials and stress relaxation. As mentioned, in the shape memory cycle to memorize the permanent shape, the hard phase is

needed to form an integrated polymeric network that stores the deformation stress and releases it during the recovery step of the shape memory cycle. Also, the responsibility of fixing the temporary shape after programming steps and recovering the applied deformation is due to the soft phase. This microscopic concept of SMPs is generalized to novel encapsulated and bilayer macroscopic designed SMP structures (PCL–TPU) using multimaterial printing. The SMP is the assembly of a non-shape memory thermoplastic (PCL) with a melting temperature and an elastomer (TPU) that is printed on the former layer. The thermoplastic is responsible for fixing the temporary shape in temperatures below its melting temperature. During the programming steps, by deforming the structure at 63 °C and cooling the structure to the ambient temperature, a portion of deformation stress is stored in the elastomer. When the structure is heated above the melting temperature of the PCL, the mentioned layer softens and leads to the release of stored stress in the TPU. PCL–TPU structures are printed with two bilayered and encapsulated designs. In addition to thermal analysis, shape memory properties are investigated with two constrained and free mechanisms to evaluate the shape fixity, shape recovery, and stress recovery in the bending and compression loading modes.

2. Experimental Section

2.1. Materials and 3D Printing

In this study, PCL and TPU filaments were prepared by the eSun company. According to the mechanical evaluation of raw materials, the flexural moduli of PCL and TPU were 345.3 ± 4.3 and 91.9 ± 3.8 MPa, respectively. The bilayer and encapsulated structure of PCL–TPU were produced using an FDM printer equipped with two nozzles. The samples were printed in two geometries: a beam with dimensions of $50 \times 10 \times 4$ mm and a cube with dimensions of 10 mm, where PCL was encapsulated by TPU. In **Figure 1**, the printed samples and their schematics are presented for two loading modes: compression and bending. To investigate the effect of the volume percentage of components, three volumes of 30%, 50%, and 70% of each component were selected without change in thickness and geometry of samples. For example, in the compression test samples, the number of the TPU cover layers was 4, 7, and 12 printing layers for 30%, 50%, and 70% encapsulated structures, respectively. TPU layers were printed at a nozzle temperature of 220 °C, a velocity of 20 mm s^{-1} , nozzle diameter of 0.8 mm, and the corresponding parameters for PCL, were 120 °C, a velocity of 40 mm s^{-1} , and nozzle diameter of 0.4 mm, respectively. The layer thickness was also considered to be 200 μm for both materials.

2.2. DMTA

DMTA test was used to perform thermal analysis and thermomechanical behavior of raw materials by a dynamic mechanical thermal analyzer (Mettler Toledo, Switzerland). The dimensions of the printed PCL and TPU were $40 \times 10 \times 1$ mm and square cube with sides of 10 mm for the bending and compression loading modes. The test was performed under bending mode in the

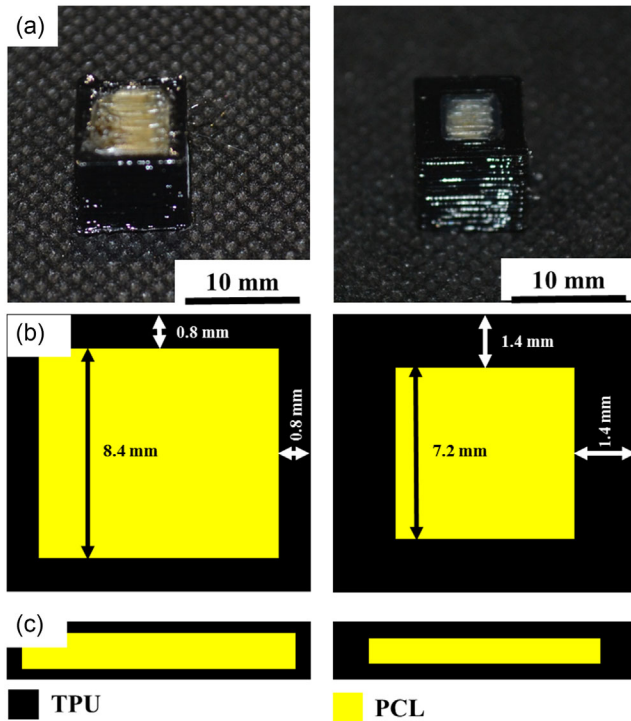


Figure 1. Cross-section of a) original and b,c) schematic-encapsulated PCL-TPU structures for compression and bending.

temperature range of -100 to 100 °C, with a fixed frequency of 1 Hz and a heating rate of 5 °C min^{-1} according to the ASTM D4065-01.

2.3. Shape Memory Effect

The shape memory effect was investigated comprehensively in two stages programming and recovery. Programming of the printed samples was done in four steps: heating, loading, cooling, and unloading. Heating was applied from ambient temperature to 55 °C at a rate of 15 °C min^{-1} and then the sample was kept at the programmed temperature for 240 s. Deformation in bending and compression modes were conducted at 7 and 4 mm, respectively. The amount of bending and compressive strain is 6.72% and 40% , respectively. After loading, the samples were quickly cooled to 25 °C at a rate of 30 °C min^{-1} and kept for 120 s. In **Figure 2**, the programming steps are presented for both the bilayer and encapsulated PCL-TPU structure in bending mode. After unloading, the amount of shape fixity was calculated by measuring the amount of storage deformation according to Equation (1). A , B , C , and D are the initial height, the amount of deformation, and the height after unloading, and recovery, respectively.

$$\text{shapefixity ratio} = \frac{B}{A - C} \times 100 \quad (1)$$

The recovery process was carried out with two free and constrained shape recovery mechanisms to obtain shape fixity, shape recovery, and stress recovery. In the free shape recovery process, the programmed samples were heated to 55 °C at a rate of

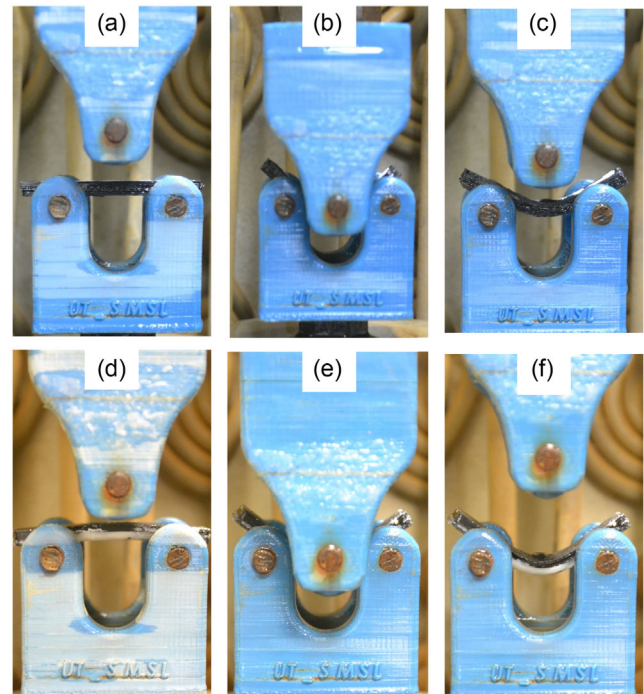


Figure 2. Programming steps including heating, loading, cooling/unloading for a-c) encapsulate and d-f) bilayer PCL-TPU structures.

15 °C min^{-1} , and after 240 s, and the measurement of the recovered shape, the amount of shape recovery was calculated based on Equation (2). The free shape memory test under bending mode was repeated for up to five cycles, and shape fixity and shape recovery values were extracted for two bilayer and encapsulated PCL50 structures.

$$\text{shape recovery ratio} = \frac{A - C}{D - C} \times 100 \quad (2)$$

The same process was repeated with the constrained shape recovery and the amount of recovered force during heating was recorded and the stress recovery was also calculated.

3. Results and Discussion

3.1. DMTA

Figure 3 shows the $\tan \delta$ curves of TPU and PCL filaments as raw materials. TPU has a wide range of glass transition phases. This transition range starts from -40 °C and continues to about 30 °C for TPU. Also, considering the highest $\tan \delta$ point as the glass transition temperature, TPU has a glass transition temperature of -1 °C. According to **Figure 3**, PCL has a narrower glass transition area than TPU in the temperature range from -65 to -30 °C. Also, the glass and melting temperatures for PCL are -60 and 60 °C, respectively. **Figure 4** demonstrates the storage modulus changes of TPU and PCL according to the temperature in the DMT test. According to these results, the middle point of the storage module can be considered as α transition temperature, which shows a value of -12 °C for TPU. The trend of

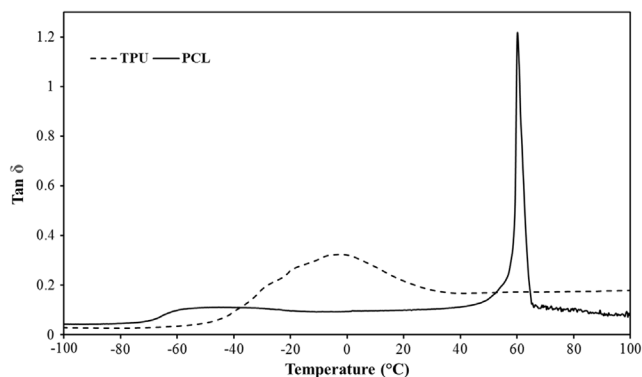


Figure 3. DMTA test result, $\tan \delta$ curves for PCL and TPU.

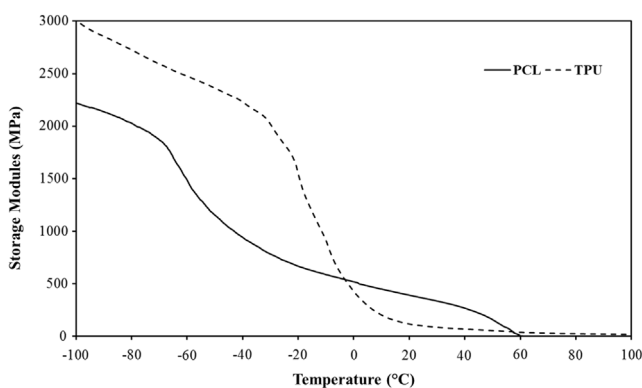


Figure 4. DMTA test result, storage modulus curves for PCL and TPU.

storage modulus changes in PCL is that it decreases from -60°C to 0° from 1497.4 to 518.9 MPa with a steep slope, and then its values at 25 and 55°C are 362.7 and 81.3 MPa, respectively. Another remarkable point is the drastic reduction of the storage modulus for PCL to less than 2 MPa at the melting region. The reduction trends of storage modulus for TPU are different and the values in the temperature range of $25\text{--}55^\circ\text{C}$ are between 99.8 and 47.8 MPa.

3.2. SME

The schematic of the new method for the shape memory behavior of bilayered FDM-printed structures is presented in Figure 5. In this method, without the primary materials having shape memory behavior, using two-material printing and using the microscopic concepts of SMPs, this method is presented. The structure of SMPs consists of two hard (net points) and soft (switching phase) segments to store energy (temporary shape) and release it (main shape) next to each other microscopically. Now, taking the idea from the microscopic structure of SMPs and the availability of producing two-material structures with 3D printing, two layers of elastomer and thermoplastic are used to assume the roles of net points and switching phase, respectively. The elastic modulus of SMPs decreases drastically at temperatures above the transition temperature and they are easily

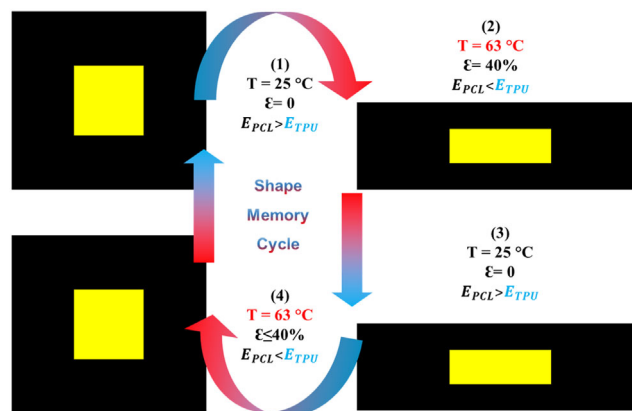


Figure 5. Schematic of samples during the shape memory cycle under compression: 1) as printed, 2) heating and loading, 3) cooling and unloading, 4) heating and recovery.

deformed to the desired extent. After cooling, the stored internal force cannot be released due to the strong increase in the elastic modulus, and the structure is maintained at a temperature lower than the transition temperature with internal force. When the SMP is heated above T_g without any external force, the internal force is released and the SMP structure recovers the original shape.^[12]

For a better understanding of the concept, the storage modulus data of the DMTA test at different temperatures have been extracted and presented in Table 1. According to Figure 5(1), the bilayer-encapsulated 3D printed structure consists of elastomer (TPU) and thermoplastic (PCL) layers. The programming temperature is considered to be the same as the thermoplastic transition temperature which is the melting temperature of PCL, and by keeping it in this thermal region, the storage modulus drops (362.7 to 2.1 MPa) drastically, so that it is possible to apply high deformation to the bilayer structure. After loading, the sample rapidly cools down to the thermoplastic glass region, which is accompanied by a sharp increase in the storage modulus (362.7 MPa), which causes the bilayer structure to fix its temporary shape. In addition, freezing the thermoplastic layer and this layer with a higher storage modulus does not allow the recovery of stored force in the elastic layer to provide the potential driving force for the recovery of the permanent shape. At this point, the storage modulus of the thermoplastic layer is 3.63 times that of TPU. Figure 5(2–3) shows the heating, loading, and cooling stages of programming, respectively. According to Figure 5(4), in the recovery stage, by reheating the temperature up to the thermoplastic transition zone, its storage modulus decreases, and the

Table 1. Storage modulus data extracted from DMT for PCL and TPU at different temperatures.

Temperature (0°)	PCL	TPU
-60	1497.4	2478.6
0	518.9	407.1
25 (Cooling)	362.7	99.8
63 (Recovery)	2.1	34.8

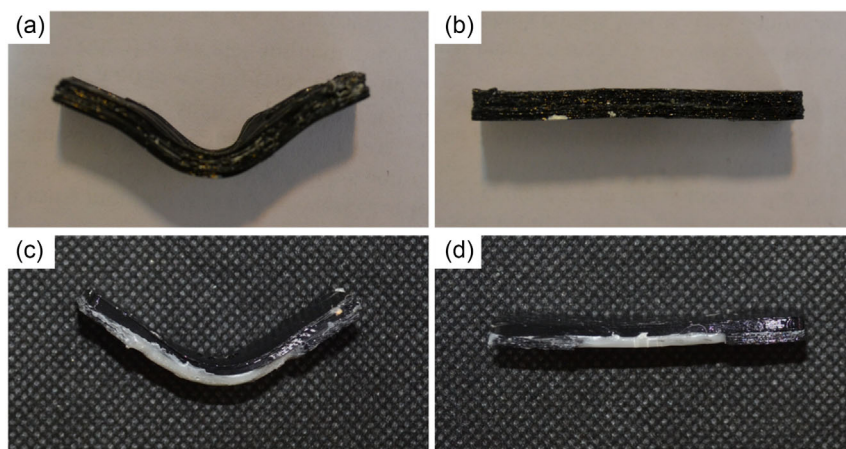


Figure 6. Programmed and recovered a,b) encapsulated and c,d) bilayer PCL50-TPU structure.

stored force in the elastic layer and permanent shape are allowed to recover. In the following, in two bending and compressive loading modes, the shape memory properties of PCL-TPU bilayer structures are comprehensively evaluated.

3.3. SME under Bending

In **Figure 6**, encapsulated and bilayer PCL-TPU structures with the same percentages of components are observed after programming and recovery under bending mode. One of the challenges

Table 2. Shape fixity and shape recovery according to the weight ratio of the components under bending loading.

Sample \ Shape state	Shape fixity	Shape recovery
PCL30	77.1	98
PCL50	85.1	100
Bilayer PCL50	77.4	100
PCL70	94.9	100

of this method in the bilayer structure is the adhesion between the thermoplastic and elastomer layers. Also, bilayer structures whose switching temperature is the melting temperature of the thermoplastic layer such as PCL are subject to melting and even destruction of the structure during loading and programming. According to **Figure 6** and the calculated results in **Table 2**, the shape fixity values for the bilayered and encapsulated PCL-TPU structures with the same component ratio (50–50) are 77.4% and 85.1%, respectively. This difference is due to the function of PCL as a barrier to prevent the relaxation of TPU after cooling and unloading, which, according to **Figure 5 (3)**, is the degradation and dripping of the molten PCL layer in water at its melting temperature. In the encapsulated structure, the TPU coating on the PCL prevents its destruction or even separation of the layers. Also, the encapsulated and bilayer PCL-TPU structures have a full shape recovery ratio—the main reason can be contributed to the very low storage modulus of PCL compared to TPU at the recovery temperature, which causes the stored force of the elastomer to be released without any resistance.

In **Figure 7**, PCL-TPU structures in three different component percentages after printing, programming, and recovery

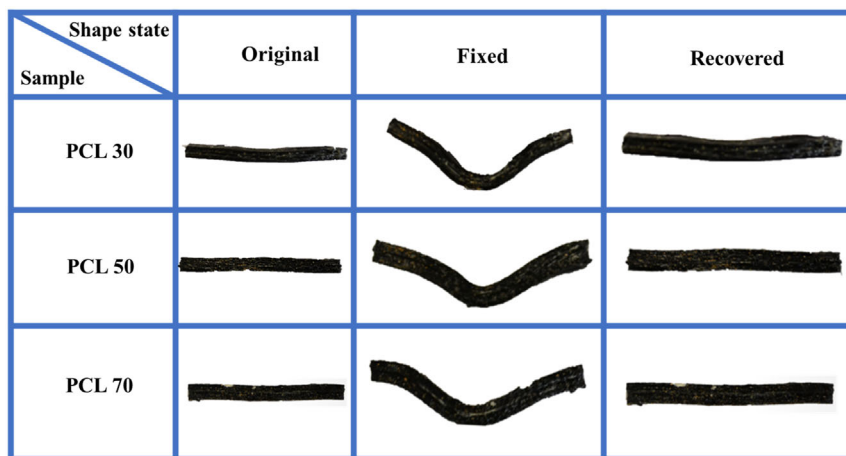


Figure 7. Original, programmed, and recovered encapsulated PCL-TPU structures according to the volume percentage of the components.

are presented. Using Equation (1) and (2), the value of fixity and shape recovery was calculated and the results are presented in Table 2. In the novel introduced strategy, the parameters affecting the shape fixity ratio are the amounts of PCL storage modulus drop in cooling temperature compared to programming temperature, as well as the ratio of PCL storage modulus to TPU in cooling temperature. PCL has a storage modulus of 2.1 MPa and 362.7 at the programming and cooling steps, respectively, which means that the transition from the molten state to glassy is complete, but at the cooling temperature, the ratio of the PCL storage modulus to TPU is about 3.63. This ratio does not provide the necessary resistance to prevent the relaxation and recovery of TPU after cooling and unloading, and for this reason, an 85.1% shape fixity ratio is obtained with the same component ratio (50–50). This storage modulus ratio in PCL–TPU structure can be controlled and manipulated by changing the thickness ratio of the layers. For this purpose, shape memory performance has been investigated for two ratios of PCL30% and PCL70%. As expected, with the increase in PCL thickness, more resistance after cooling is created and a higher shape fixity value is obtained. According to Table 2, the shape fixity ratios for the samples with the highest and lowest PCL weight percentage are 94.9% and 77.1%, respectively. The shape recovery results for all three encapsulated structures with different component ratios and even the bilayer structure are 100%, the main reason for which is the low value of the storage modulus of PCL at the recovery temperature. Also, at this temperature, the storage modulus ratio of TPU to PCL is 16.6%, and this factor is the reason for obtaining full shape recovery in all component ratios.

The results of SME according to the number of shape memory cycles under bending mode for bilayer and encapsulated PCL50 are presented in Table 3. According to the results, the best shape memory performance (both shape fixity and shape recovery) in all cycles is for the encapsulated structure. According to Table 3, the main difference in shape memory performance in the two structures is due to shape fixity values, in which the two-layer structure shape fixity decreases with the increase of shape memory cycles. The highest decreasing rate is in the second cycle, and with the increase of cycles, the decreasing rate of shape fixity performance decreases. In contrast, for the encapsulated structure, the trend of shape fixity in terms of cycles is decreasing, but at a very low rate. The amount of shape fixity in the fifth cycle is reduced by about 2% compared to the first cycle, which indicates a good shape fixity performance. As mentioned, PCL has the task of keeping TPU at the ambient temperature and directly affects the shape fixity. Since PCL is semimelted at programming

Table 3. Shape fixity and shape recovery according to the number of shape memory cycles under bending loading for bilayer and encapsulated PCL50.

Number of cycles	Shape state		Shape fixity		Shape recovery	
	Bilayer	PCL50	Bilayer	PCL50	Bilayer	PCL50
1			77.4	85.1	100	100
2			72.7	84.7	100	100
3			69.3	84.1	98.30	100
4			68.3	83.5	97.23	100
5			68.2	83.3	97.02	100

temperature, encapsulating it with TPU improves shape memory performance. The shape recovery values for both structures are significant and the same, which is due to the similar performance of the TPU layer in the recovery process. The encapsulated structure has full shape recovery in all cycles, and this value for the bilayer structure in the last cycle is 97%.

3.4. SME under Compression

In the compression loading mode, in addition to the free shape recovery evaluation, constrained recovery is also done to check the stress recovery, which is analyzed by programming and recovery stresses and shape fixity and recovery ratios.

Figure 8 presents the stress–strain diagrams for encapsulated PCL–TPU structures with different percentages of components under compression mode at the programming temperature of 63 °C. According to the results, all three samples behave with the same trend, and with the increase of the strain, the stress increases continuously. Also, the graphs have two linear curves with different slopes. One is up to 10% strain with a higher slope and the other is gentler. This behavior shows the contribution of TPU elastomer layers, which is completely different from the behavior of thermoplastics such as PCL. It is also observed that by increasing the amount of PCL in the encapsulated PCL–TPU structures, there is no change in the compression behavior and all three structures have the same stress–strain curves. As stated in the previous section, at the programming temperature, PCL has a very small elastic modulus compared to TPU, and this makes the behavior of the structures completely elastomeric.

The extracted results from the free shape memory test including shape fixity and recovery ratios for encapsulated PCL–TPU structures with different component ratios are presented in Figure 9. The shape fixity value is in the range of 64.2–75.4%, which increases with the increase of PCL value, which is consistent with the results of bending loading mode. In the programming step, the programmed stress is applied to PCL and TPU, and by cooling, the PCL and TPU layers play two completely different behaviors due to their nature. The elastic modulus of PCL increases greatly and prevents the return of the TPU layer (release of stored energy) and with the increase of PCL, a stronger constraint is created, which causes the

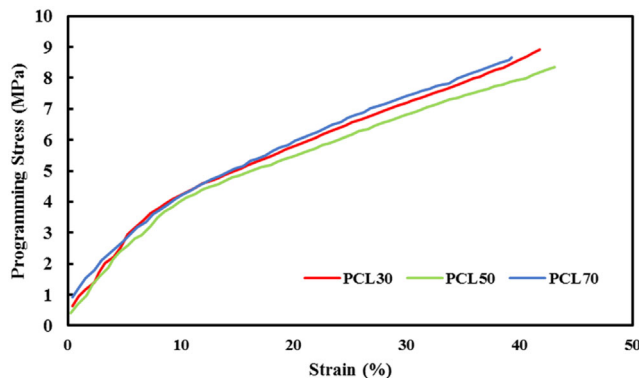


Figure 8. Stress–strain diagram for encapsulated PCL–TPU structures according to the weight percentage of components under compression loading at the programming temperature of 63 °C.

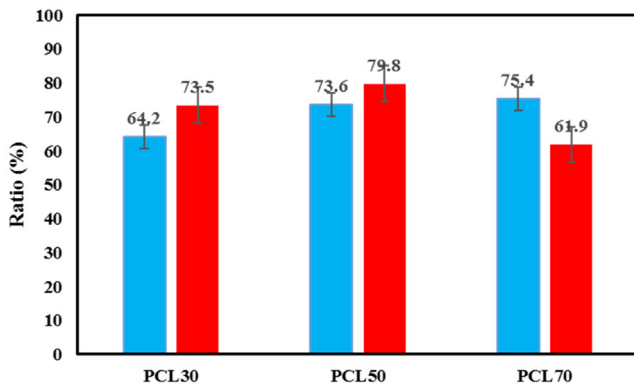


Figure 9. Shape fixity and shape recovery according to the weight ratio of the components under compression loading.

increase of the shape fixity ratio. The shape recovery values for all three encapsulated PCL-TPU structures are also shown in Figure 9. The shape recovery ratios are in the range of 61.9–79.8% and the highest recovery was obtained for PCL50.

Figure 10 shows the stress recovery diagram in terms of temperature and time for three encapsulated PCL-TPU structures with different weight percentages of the components. According to Figure 10, the amount of stress recovery increases with increasing temperature and this trend is observed in all three samples. Also, the slope of the stress increase for the samples is almost the same up to the temperature range of 50 °C, but after that, the slope of the PCL70 sample is higher, which increases due to the thinner TPU coating and also, with increasing temperature, the effect of reducing its resistance for TPU recovery increases.

In **Figure 11**, it is clear that there is stress recovery in terms of time, and the highest stress recovery value is obtained for PCL50 at the highest recovery temperature. The maximum stress recovery for PCL30, PCL50, and PCL70 are 2.26, 3.13, and 2.58 MPa, respectively. The lower stress recovery for the PCL30 sample compared to the other two samples is due to its weaker performance in the fixity value that affects the stored stress in the TPU layer. In contrast, the lower stress recovery in the PCL70 compared to PCL50 is due to the essential role of TPU in the recovery

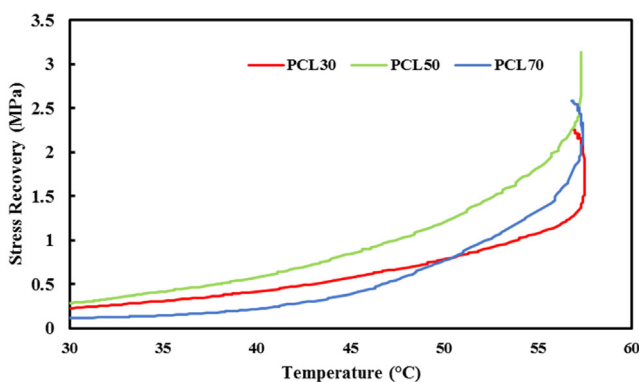


Figure 10. Stress recovery diagrams of encapsulated PCL-TPU structures in terms of temperature.

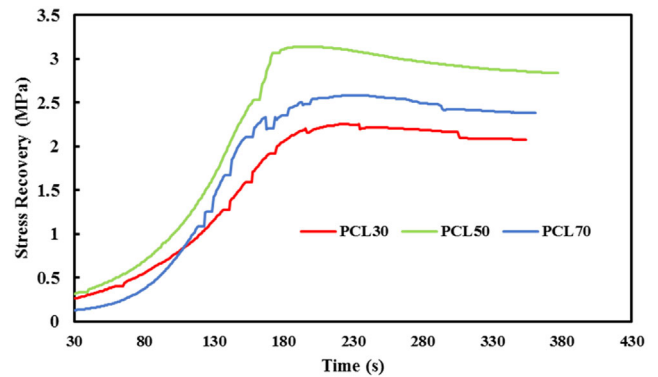


Figure 11. Stress recovery diagrams of encapsulated PCL-TPU structures in terms of time.

process, which has the main task of stress recovery during a severe drop in the PCL modulus. According to the results of the programming and shape fixity ratio (Figure 8 and 9), PCL50 has almost the same programming stress and shape fixity as PCL70. Therefore, because of the same conditions in the programming stage and the higher TPU-to-PCL ratio, PCL50 shows a better recovery performance. Figure 11 is presented to compare the relaxation of stress recovery and as can be seen, the amount of relaxation is very small for all three samples, which is also caused by the decreasing effect of time on the elastic modulus of TPU. According to the DMTA results, the elastic modulus of TPU is almost constant in the temperature range from 60 to 90 °C. In all thermoplastics that have a shape memory effect, stress relaxation is known as a major challenge and weakness due to the lack of strong net points. Thermoplastic SMPs usually have two types of physical and chemical net points, which are crystal networks and molecular entanglements, respectively. In addition, molecular entanglements in amorphous SMPs as net points have lower temperature resistance, and usually, in a short period at the transition temperature, their opening occurs which results in relaxation. One of the advantages of the introduced methods is resistance to stress relaxation which is not observed in other 4D-printed structures because stress recovery occurs by the elastic layer, in which relaxation is negligible.

4. Concluding Remarks

In this study, for the first time, novel bilayer and encapsulated shape memory structures were developed via multimaterial printing of nonshape memory polymers by fused deposition modeling 4D printing considering the microscopic structure of SMPs. The following remarks are concluded. 1) In this method, PCL, TPU, and melting temperature of PCL play the role of switching phase, net point, and transition temperature, respectively, in the shape memory cycle. The parameters affecting the shape fixity ratio were the amount of PCL storage modulus drop-in programming temperature compared to cooling temperature, as well as the ratio of PCL storage modulus to TPU in cooling temperature. 2) Due to the destruction and dripping of molten PCL in contact with water, PCL structures encapsulated by TPU were printed. In addition, the encapsulated

structures solved the challenge of bonding between the layers in the bilayer structure, and the results showed that the shape memory performance of the encapsulated structure was also better than bilayer PCL-TPU structures. 3) The shape fixity values under compression were in the range of 64.2–75.4%, which increased with the rising of PCL value, which was consistent with the results of bending loading mode. 4) At the melting temperature of PCL, the elastic modulus of TPU was 16.5 times higher than that of PCL, and the material exhibited fully elastic behavior during loading and recovery. Therefore, in the recovery process under bending, PCL was not able to resist the release of TPU force, and 100% shape recovery values were obtained in all three encapsulated and bilayered structures. 5) The results of the constrained shape memory test under compression showed that the maximum stress value was obtained at the highest temperature and for PCL30, PCL50, and PCL70 were 2.26, 3.13, and 2.58 MPa, respectively. Also, the maximum stress did not decrease with time, which indicated no stress relaxation due to the elastic behavior of the structures at the recovery temperature. 6) This novel method has two great achievements. One is the shape memory behavior without the need for SMPs, and the second is the small amount of stress relaxation compared to thermoplastic SMPs with printability by FDM. Also, the encapsulated structures have solved the limitation of adhesion between the layers, making this method applicable and universal for all commercial filaments.

Conflict of Interest

The authors declare no conflict of interest.

Data Availability Statement

All data are included in the paper.

Keywords

encapsulation, fused deposition modeling, shape memory effects, stress relaxation, 4D printing

Received: September 9, 2022

Revised: October 27, 2022

Published online:

- [1] R. Hamzehei, A. Serjouei, N. Wu, A. Zolfagharian, M. Bodaghi, *Adv. Eng. Mater.* **2022**, *24*, 2200656.

- [2] F. Momeni, S. M. M. Hassani, X. Liu, J. Ni, *Mater. Des.* **2017**, *122*, 42.
- [3] R. Akman, H. Ramaraju, S. J. Hollister, *Adv. Eng. Mater.* **2021**, *23*, 2100219.
- [4] M. Moradi, A. Aminzadeh, D. Rahmatabadi, S. A. Rasouli, *J. Mater. Eng. Perform.* **2021**, *30*, 5441.
- [5] M. Moradi, A. Aminzadeh, D. Rahmatabadi, A. Hakimi, *Mater. Res. Express.* **2021**, *8*, 035304.
- [6] M. Aberoumand, D. Rahmatabadi, A. Aminzadeh, M. Moradi, *Fused Deposition Modeling Based 3D Printing*, Springer, Cham **2021**, pp. 377–402, https://doi.org/10.1007/978-3-030-68024-4_20.
- [7] T. Sauter, K. Lützow, M. Schossig, H. Kosmella, T. Weigel, K. Kratz, A. Lendlein, *Adv. Eng. Mater.* **2012**, *14*, 818.
- [8] M. Barletta, A. Gisario, M. Mehrpouya, *J. Manuf. Process.* **2021**, *61*, 473.
- [9] J. Carrell, G. Gruss, E. Gomez, *Rapid Prototyping J.* **2020**, *26*, 855.
- [10] M. Bodaghi, A. R. Damanpack, W. H. Liao, *Smart Mater. Struct.* **2018**, *27*, 065010.
- [11] G. F. Hu, A. R. Damanpack, M. Bodaghi, W. H. Liao, *Smart Mater. Struct.* **2017**, *26*, 125023.
- [12] A. Nojiri, E. Iwase, M. Hashimoto, in *2019 IEEE 32nd Int. Conf. Micro Electro Mechanical Systems (MEMS)*, IEEE, Piscataway, NJ January 2019, 380–383. <https://doi.org/10.1109/MEMSYS.2019.8870849>.
- [13] A. Melocchi, M. Uboldi, N. Inverardi, F. Briatico-Vangosa, F. Baldi, S. Pandini, G. Scalet, F. Auricchio, M. Cerea, A. Foppoli, A. Maroni, L. Zema, A. Gazzaniga, *Int. J. Pharm.* **2019**, *571*, 118700.
- [14] E. Soleyman, M. Aberoumand, K. Soltanmohammadi, D. Rahmatabadi, I. Ghasemi, M. Baniassadi, K. Abrinia, M. Baghani, *Manuf. Lett.* **2022**, *33*, 1.
- [15] M. Aberoumand, K. Soltanmohammadi, E. Soleyman, D. Rahmatabadi, I. Ghasemi, M. Baniassadi, K. Abrinia, M. Baghani, *J. Mater. Res. Technol.* **2022**, *18*, 2552.
- [16] E. Soleyman, M. Aberoumand, D. Rahmatabadi, K. Soltanmohammadi, I. Ghasemi, M. Baniassadi, K. Abrinia, M. Baghani, *J. Mater. Res. Technol.* **2022**, *18*, 4201.
- [17] E. Soleyman, D. Rahmatabadi, K. Soltanmohammadi, M. Aberoumand, I. Ghasemi, K. Abrinia, M. Baniassadi, K. Wang, M. Baghani, *Smart Mater. Struct.* **2022**, *31*, 085002.
- [18] J. F. Mano, *Adv. Eng. Mater.* **2008**, *10*, 515.
- [19] M. Anthamatten, K. Cavicchi, G. Li, A. Wang, *J. Polym. Sci., Part B: Polym. Phys.* **2016**, *54*, 1319.
- [20] M. Carlson, Y. Li, *Int. J. Adv. Manuf. Technol.* **2020**, *106*, 4263.
- [21] X. Peng, H. He, Y. Jia, H. Liu, Y. Geng, B. Huang, C. Luo, *J. Mater. Sci.* **2019**, *54*, 9235.
- [22] S. Chen, Q. Zhang, J. Feng, *J. Mater. Chem. C.* **2017**, *5*, 8361.
- [23] H. Liu, H. He, B. Huang, *Macromol. Mater. Eng.* **2020**, *305*, 2000295.
- [24] C. Lin, L. Liu, Y. Liu, J. Leng, *Compos. Struct.* **2022**, *279*, 114729.
- [25] B. Peng, Y. Yang, T. Ju, K. A. Cavicchi, *ACS Appl. Mater. Interfaces* **2021**, *13*, 12777.